Effects of Kinetics and Optical Attenuation on the Completeness, Uniformity, and Dynamics of Monomer Conversion in Free-Radical Photopolymerizations

Guillermo Terrones*

Process Science and Engineering Department, Pacific Northwest National Laboratory, P.O. Box 999, Richland, Washington 99352

Arne J. Pearlstein*

Department of Mechanical and Industrial Engineering, University of Illinois at Urbana-Champaign, 1206 West Green Street, Urbana, Illinois 61801

Received April 19, 2001; Revised Manuscript Received September 10, 2001

ABSTRACT: For free-radical photopolymerizations with a photobleaching initiator in an initially uniform layer illuminated from one direction, we incorporate nonuniform photoinitiation into a simple kinetic model to show how the degree of monomer conversion varies spatially and temporally with the incident light intensity (I_0), the absorption coefficient (α_A) and initial concentration ($C_{A,0}$) of the photoinitiator, and the propagation (k_p) and termination (k_t) rate constants (taken to be independent of the degree of conversion). We show that the spatiotemporal variation of monomer conversion depends on two dimensionless parameters: the initial absorbance $\gamma = \alpha_A C_{A,0} L$, where L is the layer thickness, and $\beta = k_p[fC_{A,0}/(\phi\alpha_A I_0 k_t)]^{1/2}$, where ϕ is the quantum yield of photoinitiator consumption, and $0 \le f \le 2$ is the number of primary radicals produced for each photoinitiator molecule consumed. For each value of γ, there is a minimum value of β beyond which a specified layer-averaged extent of monomer conversion is assured. As β decreases, so does the extent of monomer conversion, with the final degree of conversion being lowest near the optical "front" of the layer, where the light absorption and photoinitiation rates are initially highest. The extent of nonuniformity decreases with increasing β until $\beta \approx 2$, beyond which monomer conversion is essentially complete regardless of the initial absorbance. The results are discussed in terms of the spatiotemporal distributions of the primary radical and radical chain concentrations.

Introduction

Photopolymerization in strongly absorbing or thick layers can lead to nonuniform photoinitiation and monomer conversion rates, a problem that has been recognized for many years.[1]

In an earlier paper on the effects of optical attenuation and photoinitiator consumption on spatiotemporal variation of initiation rates in systems with photobleaching initiators,[2] we discussed how spatial variation in the degree of monomer conversion and cross-linking, and other sources of heterogeneity (e.g., pools of unreacted monomer), can affect the performance of photopolymerized materials,[3−11] reviewed previous work on nonuniformity in photopolymerization, especially at high initial absorbance (e.g., high initiator concentration or deep layers), and presented detailed results on the spatiotemporal variation of the concentration of a photobleaching initiator as well as the photoinitiation rate. Here, we focus on the completeness, uniformity, and rate of monomer conversion in free-radical photopolymerizations in such systems.

Standard treatments of free-radical photopolymerization kinetics do not deal with the spatiotemporal variation of initiator or monomer concentrations. If one neglects variation in these concentrations, the correct expression for the local monomer conversion rate is given by eq 6 of ref 2. Under these conditions, the correct layer-averaged monomer conversion rate

$$\bar{R}_p = 2k_p[M]\sqrt{\phi I_0/(\alpha_A[A]k_t)}(1 - e^{-\alpha_A[A]L/2})/L \quad (1)$$

is obtained by integrating the local rate over the layer thickness L and dividing by L, where ϕ is a quantum yield for the photoinitiation reaction, α_A is the absorption coefficient of the photoinitiator, [A] and [M] are the photoinitiator and monomer concentrations, respectively, and k_p and k_t are the propagation and termination rates, respectively. (Here, k_t is the termination rate constant used in ref 2 as well as by Odian[12] and other textbook authors. As discussed below, it differs by a factor of 2 from the termination rate constant used in more advanced treatments and in the present paper.) The commonly used expression[12−14]

$$\bar{R}_p = k_p[M]\sqrt{\phi I_0(1 - e^{-\alpha_A[A]L})/k_t} = k_p[M]\sqrt{\phi I_0(1 - 10^{-\epsilon_A[A]L})/k_t} \quad (2)$$

for the layer-averaged monomer conversion rate is wrong on two counts. First, since the local rate of monomer conversion is proportional to the square root of the local photon absorption rate, the layer-averaged monomer conversion rate must be obtained by averaging the square root rather than by taking the square root of an average quantity (note that the third factor under the radical in (2) is proportional to the volumetric photon absorption rate averaged over the layer thick-

* To whom correspondence should be addressed.

10.1021/ma010678e CCC: $20.00
Published on Web 11/20/2001

Table 1.

symbol	quantity	definition	units
b	layer depth or position in layer		m
C_j	concentration of species j		M
$C_{j,0}$	initial concentration of species j		M
f	number of primary radicals created per photoinitiator molecule consumed		
I	light intensity		einsteins m^{-2} s^{-1}
I_0	incident light intensity		einsteins m^{-2} s^{-1}
k_p	propagation rate constant		M^{-1} s^{-1}
k_t	termination rate constant	$k_{t,m,n}$ $(m \neq n)$	M^{-1} s^{-1}
$k_{t,m,n}$	termination rate constant for reaction of $RM_m^\bullet$ and $RM_n^\bullet$		M^{-1} s^{-1}
L	layer depth		m
R_i	initiation rate		M s^{-1}
R_p	local polymerization rate		M s^{-1}
$\bar{R}_p$	layer-averaged polymerization rate		M s^{-1}
S_j	dimensionless concentration of species j	$C_j/C_{j,0}$	
$\bar{S}_j$	layer-averaged dimensionless concentration of species j		
x	dimensional coordinate		m
z	dimensionless coordinate	x/L	
α_A	absorption coefficient of photoinitiator		M^{-1} m^{-1}
β	dimensionless parameter	$k_p[fC_{A,0}/(\phi\alpha_A I_0 k_t)]^{1/2}$	
γ	initial absorbance	$\alpha_A C_{A,0} L$	
Δ_M	back-to-front difference in dimensionless final monomer conversion		
ϵ_A	extinction coefficient of photoinitiator		M^{-1} m^{-1}
τ	dimensionless time	$\phi I_0 \alpha_A t$	
ϕ	quantum yield of initiator consumption		

ness, $I_0(1 - 10^{-\epsilon_A[A]L})/L$). That (2) is wrong is verified even more easily by considering the limit $L \rightarrow \infty$, for which (2) gives a nonzero layer-averaged monomer conversion rate, even though that quantity must vanish as $L \rightarrow \infty$ since virtually no absorption occurs beyond some "optical penetration depth". Note that in this limit (1) has the correct asymptotic behavior. Second, (2) is dimensionally inconsistent, with the right-hand side having units of M $cm^{1/2}$ s^{-1}. Consequently, no expression of the form (2) can properly account for how spatial variation in the photon absorption rate contributes to the overall monomer conversion rate, even when the photoinitiator and monomer concentrations are uniform. A similar expression for the initial photopolymerization rate (eq 5 of ref 14) is dimensionally inconsistent with both the local rate (M s^{-1}) and global rate (mol s^{-1} or mol cm^{-2} s^{-1}) of photopolymerization.

Beyond the limitations inherent in the assumptions of monochromatic illumination and quasi-steady radical chain kinetics, any approach based on neglecting spatiotemporal variation in photoinitiator and monomer concentration profiles necessarily suffers from failure to account for nonuniform consumption of photoinitiator as well as nonuniformity of the initiation rate.[2]

Several authors[6−9] have experimentally assessed effects of photoinitiator concentration and light intensity on the overall rate and final degree of monomer conversion and discussed how these factors—exposure time, attenuation, and inhibitor and photosensitizer concentrations—affect depth of cure. The importance of attenuation to spatial variation of conversion has been identified in dental applications,[7−11,15] including in situ restoration of caries, denture fabrication, and elastomeric impressioning of teeth and oral mucosal surfaces. Monomer conversion in these thick-section applications is critical for two reasons. First, depth-resolved measurements show that hardness (which is directly related to monomer conversion) depends strongly on photoinitiator concentration and incident light intensity. Second, especially in in situ restoration or removable prostheses, potentially toxic in-service elution[15−17] of unconverted monomer is a concern. Inadequate depth of cure has been linked clinically to retention failure, leakage, and caries.[4]

More generally, Mateo et al.[18] discussed how nonuniform photoinitiation can affect the molecular weight distribution, which like other quantities not predicted by simple kinetic models, is expected to depend on whether account is taken of attenuation and photoinitiator consumption. In addition, several models of monomer conversion in free-radical photopolymerizations initiated by photobleaching initiators have been considered that are essentially identical to the one considered here. One model of Shultz and Joshi[19] (for an "unstirred" photobleaching initiator, i.e., with no mass transfer) is mathematically identical to ours. For that model, they presented a closed-form solution equivalent to our solution for the monomer concentration (eq 18) but showed results only for the initial polymerization rate. They presented no numerical or graphical results for the spatiotemporal variation of monomer concentration or conversion rate, temporal variation of the corresponding layer-integrated quantities, or the final conversion of monomer. Recent work by Ivanov and Decker[20] also considers the spatiotemporal variation of monomer conversion for a model mathematically identical to ours. They present results for a single set of parameter values (termination and propagation rate constants, incident light intensity, photoinitiator concentration, quantum yield of photoinitiator decomposition appropriate to free-radical photopolymerization of acrylate monomers) but do not identify the two dimensionless parameters upon which the solution depends, and hence provide no insight into how the results depend on parameters.

Here, we use the results of our earlier work on nonuniform photoinitiation[2] as a foundation to study the completeness, uniformity, and dynamics of monomer conversion for free-radical photopolymerizations, employing a standard kinetic model in which the propagation and termination rate constants are taken to be independent of the degree of conversion. Beyond the insight that the calculations provide for systems of practical interest, they also provide a benchmark to which results for more complex kinetics (e.g., accounting for autoacceleration and autodeceleration) can be compared.

Model

We consider a mechanism[21,22]

$$\mathrm{A} \xrightarrow{h\nu} f\,\mathrm{R}^{\bullet} \tag{3}$$

$$\mathrm{R}^{\bullet} + \mathrm{M} \xrightarrow{k_p} \mathrm{RM}^{\bullet} \tag{4}$$

$$\mathrm{RM}_m^{\bullet} + \mathrm{M} \xrightarrow{k_p} \mathrm{RM}_{m+1}^{\bullet} \quad m \geq 1 \tag{5}$$

$$\mathrm{RM}_m^{\bullet} + \mathrm{RM}_n^{\bullet} \xrightarrow{k_{t,m,n}} \mathrm{RM}_{m+n}\mathrm{R} \quad m, n \geq 0 \tag{6}$$

in which all light absorption is by the photoinitiator A. We assume that the chain initiation and propagation reactions (4) and (5), respectively, have the same rate constant k_p, which together with the like and unlike termination rate constants $k_{t,n,n}$ and $k_{t,m,n}$ ($m \neq n$), respectively, are independent of both chain length and the degree of conversion of the monomer, M. The factor f accounts for the possibility that photolysis of the initiator gives rise to one or two primary radicals as well as the possibility that not all primary radicals initiate chains. Accounting for the possibility that termination can occur by reactions other than recombination, such as disproportionation, has no effect on the monomer conversion rate. We assume that the process is isothermal.

Neglecting diffusion[23] and convection[24,25] which sometimes occur in photopolymerizations, we obtain the kinetic equations

$$\frac{\partial C_A}{\partial t} = -\phi\alpha_A I(x,t) C_A \tag{7a}$$

$$\frac{\partial C_{R\bullet}}{\partial t} = f\phi\alpha_A I(x,t) C_A - k_p C_M C_{R\bullet} - 2k_{t,0,0} C_{R\bullet}^2 - \sum_{n=1}^{\infty} k_{t,0,n} C_{R\bullet} C_{RM_n\bullet} \tag{7b}$$

$$\frac{\partial C_{RM_m\bullet}}{\partial t} = k_p C_M [C_{RM_{m-1}\bullet} - C_{RM_m\bullet}] - C_{RM_m\bullet} \sum_{\substack{n=0 \\ n\neq m}}^{\infty} k_{t,m,n} C_{RM_n\bullet} - 2k_{t,m,m} C_{RM_n\bullet}^2 \quad m \geq 1 \tag{7c}$$

$$\frac{\partial C_M}{\partial t} = -k_p C_M \sum_{n=0}^{\infty} C_{RM_n\bullet} \tag{7d}$$

$$\frac{\partial C_{RM_mR}}{\partial t} = \sum_{n=0}^{[m/2]} k_{t,n,m-n} C_{RM_n\bullet} C_{RM_{m-n}\bullet} \quad m \geq 0 \tag{7e}$$

where $[m/2]$ is the largest integer not exceeding $m/2$, and $C_{RM_0\bullet}$ and $C_{R\bullet}$ both represent the primary radical concentration. Defining $k_t = k_{t,m,n}$ for $m \neq n$, we take $k_{t,m,m} = k_t/2$, as discussed elsewhere,[21,22] and note from (6) that $k_{t,m,n} = k_{t,n,m}$. Here, α_A is the wavelength-dependent absorption coefficient[26] of the photoinitiator, C_j is the molar concentration of species j, and the dependence of the light intensity $I(x,t)$ on position and time is explicitly indicated. (We note that k_t differs by a factor of 2 from the termination rate constant used in eqs 1 and 2, in ref 2 and by Odian[12] and other authors of popular textbooks but is identical to the termination rate constants used in more careful treatments.[21,22])

We consider a one-dimensional layer of thickness L subject to uniform illumination normal to the surface at $z = 0$, as in ref 2. As in our earlier work,[2] we assume that the photoinitiator is photobleached by conversion to moieties transparent at the actinic wavelength. Photobleaching photoinitiators are particularly attractive because they allow thick sections (up to several centimeters) to be cured rapidly.[3,28] We also assume that at each wavelength the light intensity decreases along the beam direction according to the integrated form of Beer's law

$$I(x,t) = I_0 \exp[-\alpha_A \textstyle\int_0^x C_A(x',t)\,dx'] \tag{8}$$

where I_0 is the incident light intensity at the optical entrance.

We assume that at $t = 0$ the concentrations of photoinitiator and monomer are uniform throughout the layer and that no other light-absorbing or reactive species are present. Thus,

$$C_A(x,0) = C_{A,0} \tag{9a}$$

$$C_M(x,0) = C_{M,0} \tag{9b}$$

We make the conventional steady-state approximation for the radical concentrations.[1,21,22] This requires that the time to establish a quasi-steady radical concentration is small compared to the time scales for photoinitiator consumption and monomer conversion, an approximation that is usually a good one. (A situation in which this not the case is considered in the Discussion.) Summing the left-hand sides of (7b) and (7c) gives

$$\frac{\partial}{\partial t} \sum_{m=0}^{\infty} C_{RM_m\bullet} = f\phi\alpha_A I(x,t) C_A - k_t \sum_{m=0}^{\infty} C_{RM_m\bullet} \sum_{n=0}^{\infty} C_{RM_n\bullet} \tag{10}$$

Making the steady-state approximation, we get the total radical concentration

$$\sum_{m=0}^{\infty} C_{RM_m\bullet} = \sqrt{f\phi\alpha_A I(x,t) C_A / k_t} \tag{11}$$

from which it follows that

$$\frac{\partial C_M}{\partial t} = -k_p \sqrt{f\phi\alpha_A I(x,t) C_A / k_t}\; C_M \tag{12}$$

Thus, within the limitations of the steady-state hypothesis on the total radical concentration, the local conversion of monomer can be determined from the solution of (7a) and (12), subject to the initial conditions (9a,b). We note that since monomer is consumed by (4) as well as (5), derivation of (12) requires that the summation in (11) begin with $m = 0$ (corresponding to the primary radical concentration).

To nondimensionalize these equations, we introduce dimensionless time $\tau = \phi I_0 \alpha_A t$, position $z = x/L$, and concentrations $S_j = C_j/C_{j,0}$ (j = A, M) along with the dimensionless initial absorbance $\gamma = \alpha_A C_{A,0} L$. As discussed earlier,[2,29] the dimensionless photoinitiator concentration is given in terms of these variables by

$$S_A = [1 + e^{-\gamma z}(e^{\tau} - 1)]^{-1} \tag{13}$$

while the dimensional local rate of formation of primary radicals is given by

$$R_i = f\phi\alpha_A I C_A = \frac{f\phi\alpha_A I_0 e^{\tau-\gamma z} C_{A,0}}{[1 + e^{-\gamma z}(e^{\tau} - 1)]^2} \tag{14}$$

We note that the local value of the total radical concentration (11) is proportional to the square root of the photoinitiation rate (14), a quantity whose spatiotemporal variation (including traveling-wave behavior at large values of the initial absorbance) was discussed thoroughly in our earlier work.[2]

The dimensionless kinetic equation for the monomer concentration can then be written as

$$\frac{\partial S_M}{\partial \tau} = -\beta \frac{e^{(\tau-\gamma z)/2}}{1 + e^{-\gamma z}(e^{\tau} - 1)} S_M \tag{15}$$

subject to the initial condition

$$S_M(z,0) = 1 \tag{16}$$

where

$$\beta = k_p\left[\frac{fC_{A,0}}{\phi\alpha_A I_0 k_t}\right]^{1/2} \tag{17}$$

The spatiotemporal variation of the monomer conversion is thus seen to depend on two dimensionless parameters, β and γ, and can be computed as the solution of the linear differential equation (15) subject to the initial condition (16). Equation 15 is essentially an ordinary differential equation (in time) for $S_M(z,\tau)$ whose solution is *parametrized* by the spatial coordinate z. Note that since no derivatives with respect to z appear in (15), it is not a partial differential equation. Since both β and γ depend on $C_{A,0}$ and α_A, it will prove useful to think of β as a kinetic parameter, focusing on its dependence on the incident light intensity I_0 and rate constants k_p and k_t, none of which appears in γ.

The solution of (15) subject to (16) is given by

$$S_M(z,\tau) = \exp\left\{-\frac{2\beta}{(1 - e^{-\gamma z})^{1/2}} \arctan\left[\frac{(e^{\gamma z} - 1)^{1/2}(e^{\tau/2} - 1)}{e^{\gamma z} - 1 + e^{\tau/2}}\right]\right\} \tag{18}$$

as can be verified by substitution. This solution is equivalent to but different in form from eq 16 of Shultz and Joshi.[19]

In what follows, it will sometimes prove convenient to express results in terms of the fractional consumption of photoinitiator $1 - \bar{S}_A$ or fractional conversion of monomer $1 - \bar{S}_M$, where the mean dimensionless concentrations averaged over the thickness of the layer are defined by

$$\bar{S}_i(\tau) = \int_0^1 S_i(z,\tau)\, dz \quad i = A, M \tag{19}$$

Results

Spatiotemporal Variation of Monomer Conversion. Evaluation of the analytical solution (18) for a wide range of the parameters β and γ shows that spatial variation of monomer conversion at the end of reaction, and spatiotemporal variation during the course of reaction, can both be significant. The implications are explored in the Discussion.

For fixed values of the kinetic parameter β and initial absorbance, we present results at several values of the photoinitiator consumption or monomer conversion. The values of β and γ considered cover the entire range of behavior. The initial absorbance ranges from 1 (where effects of attenuation and departures from uniformity are relatively small) up to 100 (for which pronounced traveling-wave behavior is predicted). We consider values of β ranging from 10^{-3} to 100. We note that β and γ in most applications fall within these ranges. The kinetic parameter β is typically 0.01−1 when differential scanning calorimetry (DSC) is used in kinetic studies of photopolymerizations, but can be much higher in other situations (e.g., ∼80 in Bowman and Peppas' work[30] at their "baseline" light intensity of 0.2 mW cm^{-2}). The initial absorbance γ is typically less than unity in DSC applications but can be considerably higher (∼600 in the work of Hutchinson and co-workers[31]).

For $\beta = 10^{-3}$ and $\gamma = 1$, Figure 1a shows monomer concentration profiles at six values of $1 - \bar{S}_A$. The monomer profiles are quite uniform, and for this small value of β the final conversion is very small. Monomer concentration increases monotonically with depth due to optical attenuation for small degrees of photoinitiator consumption, but decreases monotonically with depth at the final state (complete consumption of photoinitiator). At higher degrees of photoinitiator consumption, monomer concentration decreases monotonically with depth since conversion during the early stages of the process occurs preferentially near $z = 0$, under conditions where the photoinitiator concentration is highest, and the total radical concentration (11) is higher there than anywhere else at any time. Thus, during the initial period, a smaller percentage of the radicals created in the rear are lost at small chain length to (second-order) termination than up front, giving rise to more monomer conversion per absorbed photon in the rear than upbeam. For $\beta = 10^{-3}$ and $\gamma = 1$, less than 0.22% of the monomer in the layer has been converted at completion of the reaction.

For the same small value of β, Figure 1b,c shows that as the initial absorbance increases to $\gamma = 5$ and 10, the degree of monomer conversion becomes increasingly nonuniform. Application of L'Hôpital's rule to (18) shows that at $z = 0$

$$S_M(0,\tau) = \exp[-2\beta(1 - e^{-\tau/2})] \tag{20}$$

is independent of γ. For both of these values of γ, there is a broad range of fractional photoinitiator consumption for which the monomer concentration is a nonmonotonic function of the depth z.

At $\gamma = 100$, the wave nature of the process is clear (Figure 1d), with photoinitiator being rapidly consumed near $z = 0$ (where the monomer concentration quickly approaches its final value) and monomer being converted in a right-going wavelike process reminiscent of traveling-wave photoinitiator consumption[2] and traveling-wave photolysis of phenyl azide.[32] Even at $\gamma = 100$, the overall conversion of monomer is only about 0.31%. We also note that, beyond a region near $z = 0$, the final degree of monomer conversion is higher and essentially independent of depth. The monomer conversion up front

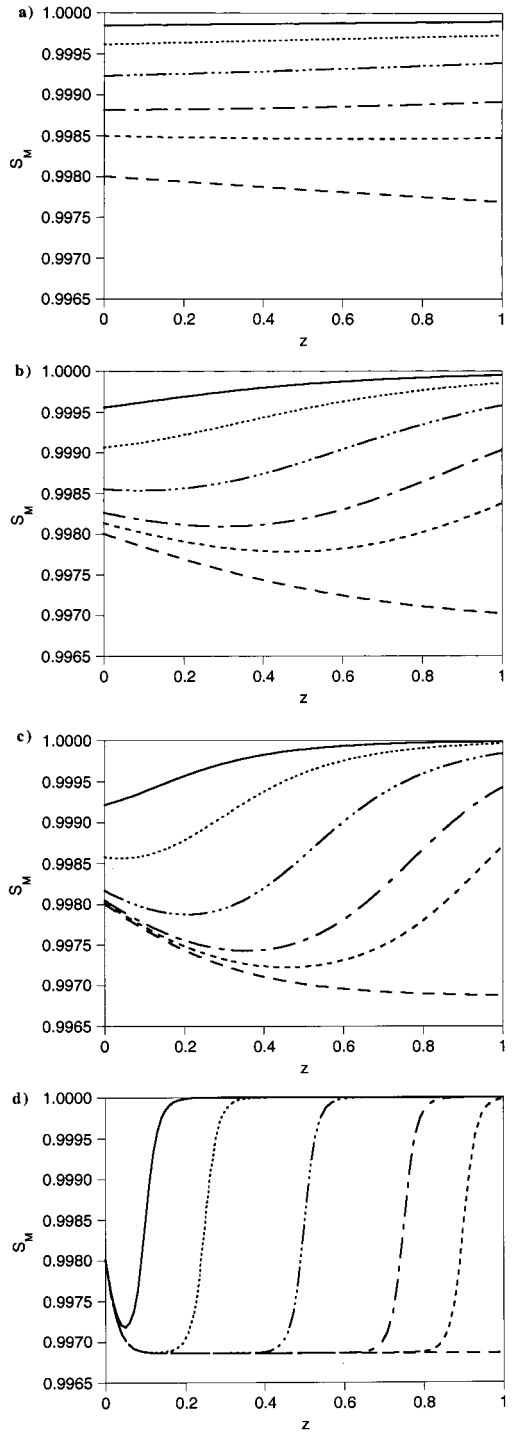

Figure 1. Spatiotemporal variation of dimensionless monomer concentration profiles $S_M = C_M/C_{M,0}$ as functions of $z = x/L$ for $\beta = 10^{-3}$ at different degrees of photoinitiator consumption $1 - \bar{S}_A$: (—) $\bar{S}_A = 0.9$; (• • •) $\bar{S}_A = 0.75$; (—• • •—) $\bar{S}_A = 0.5$; (— • —) $\bar{S}_A = 0.25$; (---) $\bar{S}_A = 0.1$; (— — —) $\bar{S}_A = 0$. (a) $\gamma = 1$; (b) $\gamma = 5$; (c) $\gamma = 10$; (d) $\gamma = 100$.

is lower because essentially no monomer there is converted under conditions of low radical chain concentration. As expected for an attenuation-related phenomenon, this region becomes increasingly localized near $z = 0$ as γ increases.

For $\beta = 0.1$, Figure 2a−d shows that at each degree of photoinitiator consumption, $S_M(z,\tau)$ is smaller than for $\beta = 10^{-3}$. The final fractional conversions of monomer range from 19.4% at $\gamma = 1$ up to 26.7% at $\gamma = 100$. The degree of nonuniformity at each stage again increases with increasing γ, with the wavelike character becoming clear at $\gamma = 100$.

For $\beta = 1$, Figure 3a−d shows that at each value of $1 - \bar{S}_A$ the degree of monomer conversion is again higher than for smaller β. A striking difference is that the final degree of monomer conversion is in excess of 88%, even at the lowest initial absorbance considered. At the highest initial absorbance ($\gamma = 100$), over 95% of monomer is ultimately converted. The larger conversions, compared to those for smaller β, can be thought of as associated with an increased value of the propagation rate constant k_p or decreased values of the termination rate constant k_t or incident intensity I_0 (see (17) et seq.). The monomer conversion increases with γ because a larger fraction of the conversion occurs under conditions of relatively low local photoinitiation rate, so that the radical chain concentration is low and termination is inefficient compared to propagation.

For $\beta = 10$, Figure 4a−d shows monomer conversion profiles for six values of $1 - \bar{S}_M$. For $\gamma = 1$, each profile is approximately linear, with the extent of photoinitiator consumption, $1 - \bar{S}_A$, being 0.9915, 0.9769, 0.9445, 0.8895, 0.8181, and 0.6480 for $1 - \bar{S}_M$, 0.75, 0.5, 0.25, 0.1, and 0.01, respectively. For $\gamma = 5$, the profiles are much less linear, the degree of photoinitiator consumption (0.9942, 0.9834, 0.9565, 0.9015, 0.8197, and 0.6292 for the same values of $1 - \bar{S}_M$) is slightly higher at all monomer conversions except the highest, and unreacted monomer is much more localized near the rear of the layer. As the initial absorbance increases further, the degree of photoinitiator consumption at comparable stages of monomer conversion increases rapidly. For example, at 99% monomer conversion, 55% of the photoinitiator has been consumed for $\gamma = 10$, while 92.8% has been consumed for $\gamma = 100$. This rapid increase in photoinitiator consumption, corresponding to much less efficient use of photoinitiator at high values of the initial absorbance, is associated with the fact that as γ increases, attenuation ensures that progressively less absorption occurs "downbeam" of the propagating wave. As a result, almost all of the upbeam photoinitiator must be consumed before monomer in the rear of the layer can be converted.

For $\beta = 100$, Figure 5a−d shows that the profiles of monomer conversion at several values of $1 - \bar{S}_M$ are quite similar to those for $\beta = 10$. A significant difference, however, is that the fractional photoinitiator consumption required to achieve a given level of monomer conversion decreases rapidly as β increases. For example, at $\gamma = 1$, only 3.8% of the photoinitiator is consumed during conversion of 99% of the monomer when $\beta = 100$, as opposed to 35% for $\beta = 10$ at the same value of γ. At $\gamma = 100$, only 88% of photoinitiator is consumed in converting 99% of the monomer, compared to 92.8% for $\beta = 10$. This more efficient use of photoinitiator is associated with the larger value of $k_p/k_t^{1/2}$.

Final Layer-Averaged Monomer Conversion. Central to photopolymerization process design is the question of what fraction of monomer is ultimately converted for a given combination of initial photoinitiator concentration, light intensity, and layer thickness. In dimensionless terms, one seeks the dependence of $1 - \bar{S}_M(\infty)$ on β and γ. The spatiotemporal profiles of monomer conversion presented above show that for sufficiently small β photoinitiator consumption proceeds with essentially no conversion of monomer. For large

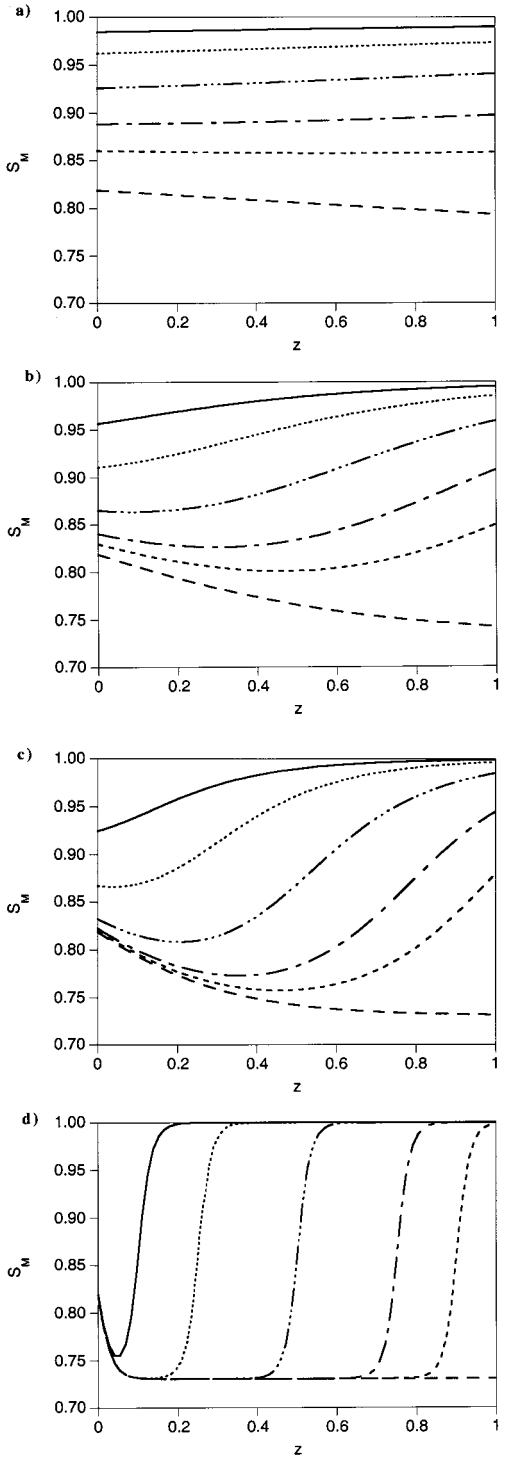

Figure 2. Spatiotemporal variation of dimensionless monomer concentration profiles $S_M = C_M/C_{M,0}$ as functions of $z = x/L$ for $\beta = 0.1$ at different degrees of photoinitiator consumption $1 - \bar{S}_A$: (—) $\bar{S}_A = 0.9$; (• • •) $\bar{S}_A = 0.75$; (—• • •—) $\bar{S}_A = 0.5$; (— • —) $\bar{S}_A = 0.25$; (---) $\bar{S}_A = 0.1$; (— — —) $\bar{S}_A = 0$. (a) $\gamma = 1$; (b) $\gamma = 5$; (c) $\gamma = 10$; (d) $\gamma = 100$.

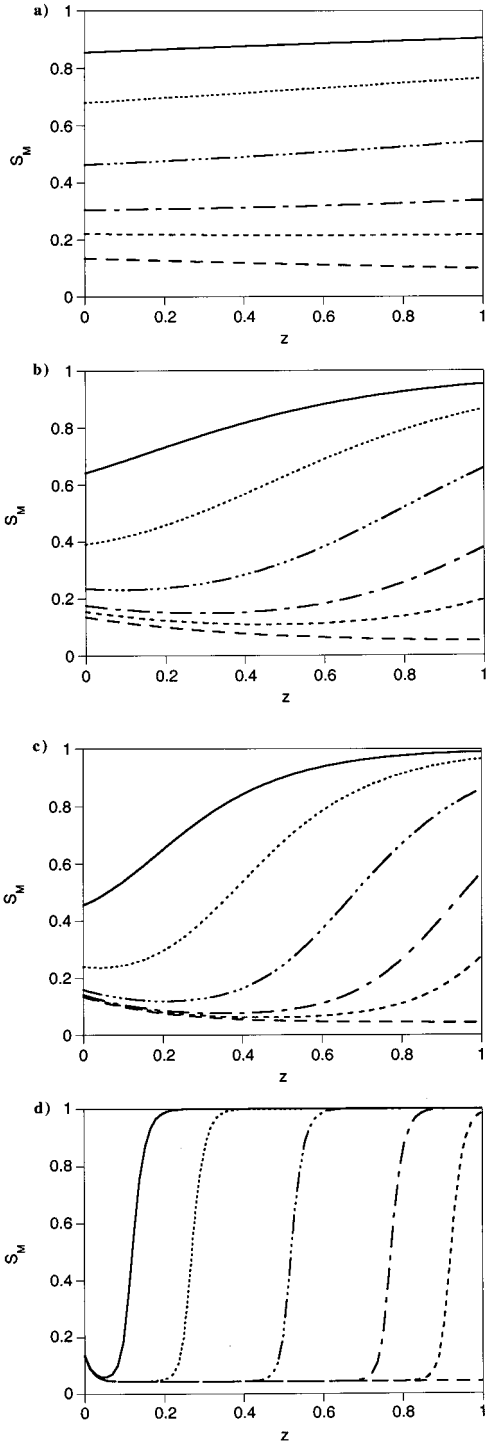

Figure 3. Spatiotemporal variation of dimensionless monomer concentration profiles $S_M = C_M/C_{M,0}$ as functions of $z = x/L$ for $\beta = 1$ at different degrees of photoinitiator consumption $1 - \bar{S}_A$: (—) $\bar{S}_A = 0.9$; (• • •) $\bar{S}_A = 0.75$; (—• • •—) $\bar{S}_A = 0.5$; (— • —) $\bar{S}_A = 0.25$; (---) $\bar{S}_A = 0.1$; (— — —) $\bar{S}_A = 0$. (a) $\gamma = 1$; (b) $\gamma = 5$; (c) $\gamma = 10$; (d) $\gamma = 100$.

β, essentially all monomer is converted. Here, we present results showing the dependence of $1 - \bar{S}_M(\infty)$ on β and γ.

Consistent with Figures 1−5, Figure 6 shows that the final degree of monomer conversion increases monotonically with β and γ and increases rapidly from $\beta = 10^{-2}$ to 1. Results for each value of γ are qualitatively similar, with the conversion increasing as γ increases. At each β, the predicted conversion differs by less than 0.12 between $\gamma = 1$ and 100, with the difference rapidly decreasing as β approaches 2 from below. As discussed above, the increase of $1 - \bar{S}_M(\infty)$ with β can be thought of as due to a higher propagation rate or a lower termination rate or light intensity.

In applications where hardness, strength, or other properties depend on the degree of monomer conversion, it is important to know how the minimum local degree of conversion depends on the parameters. Since $S_M(z,\infty)$ decreases monotonically from $z = 0$, its maximum value

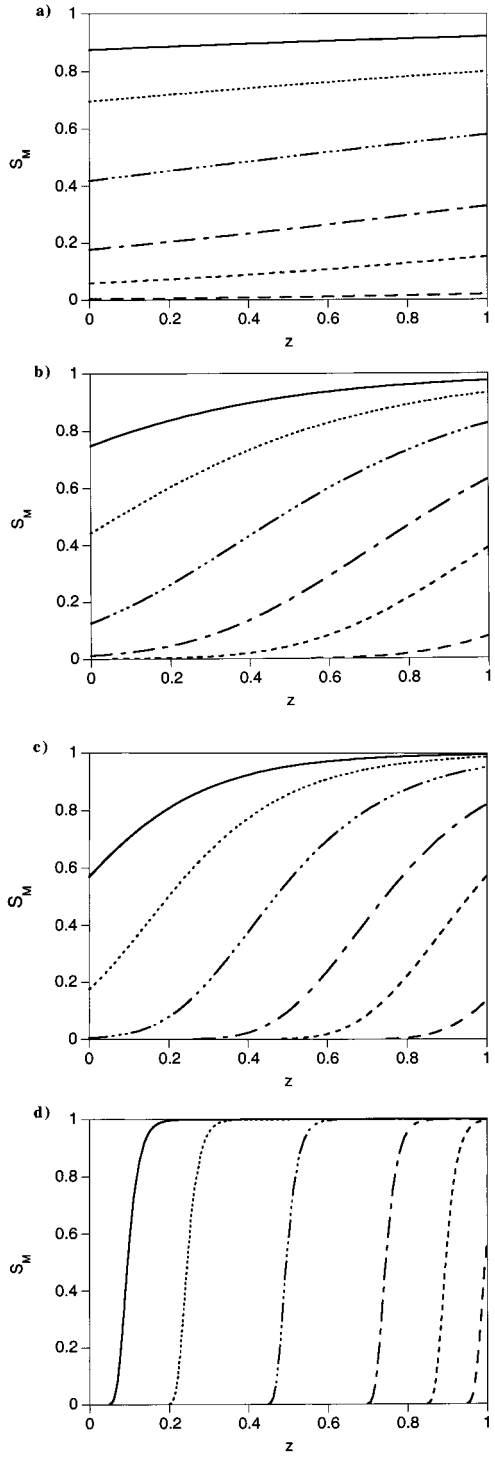

Figure 4. Spatiotemporal variation of dimensionless monomer concentration profiles $S_M = C_M/C_{M,0}$ as functions of $z = x/L$ for $\beta = 10$ at different degrees of monomer conversion $1 - \bar{S}_M$: (—) $\bar{S}_M = 0.9$; (• • •) $\bar{S}_M = 0.75$; (—• • •—) $\bar{S}_M = 0.5$; (— • —) $\bar{S}_M = 0.25$; (---) $\bar{S}_M = 0.1$; (— — —) $\bar{S}_M = 0.01$. (a) $\gamma = 1$; (b) $\gamma = 5$; (c) $\gamma = 10$; (d) $\gamma = 100$.

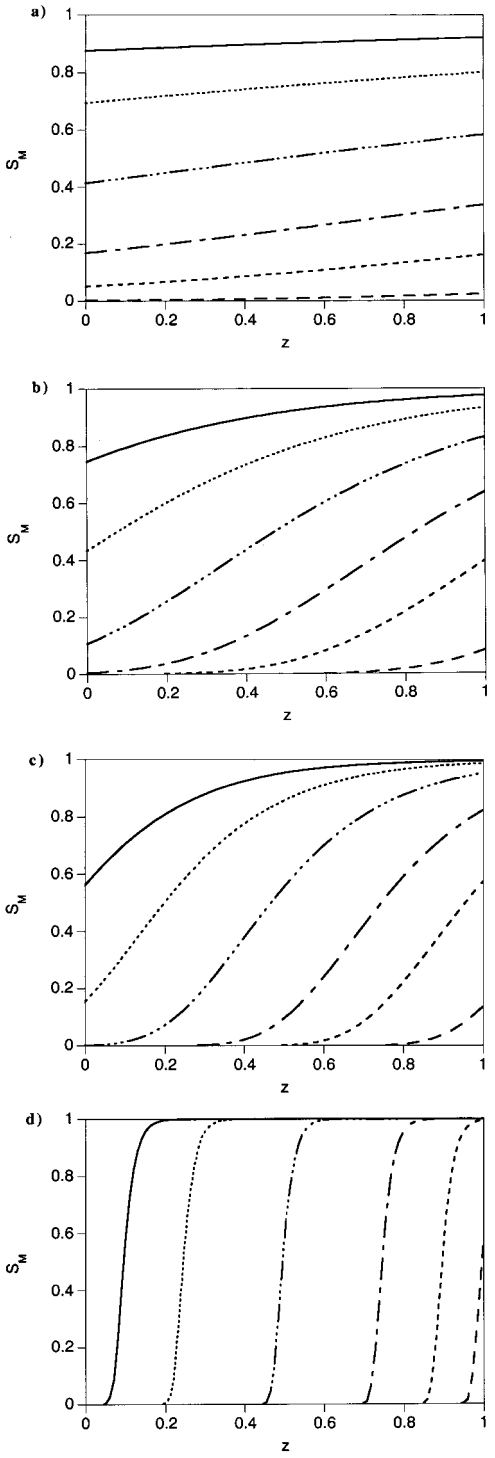

Figure 5. Spatiotemporal variation of dimensionless monomer concentration profiles $S_M = C_M/C_{M,0}$ as functions of $z = x/L$ for $\beta = 100$ at different degrees of monomer conversion $1 - \bar{S}_M$: (—) $\bar{S}_M = 0.9$; (• • •) $\bar{S}_M = 0.75$; (—• • •—) $\bar{S}_M = 0.5$; (— • —) $\bar{S}_M = 0.25$; (---) $\bar{S}_M = 0.1$; (— — —) $\bar{S}_M = 0.01$. (a) $\gamma = 1$; (b) $\gamma = 5$; (c) $\gamma = 10$; (d) $\gamma = 100$.

must occur at $z = 0$. From (20) it then follows that the maximum unconverted monomer fraction at any depth in the layer is $e^{-2\beta}$. Thus, the minimum value of β required to guarantee that the unconverted monomer fraction nowhere exceeds a specified level S^*_M is $\beta^* = -(\ln S^*_M)/2$.

Nonuniformity of Final Monomer Conversion. Beyond the overall extent of monomer conversion, a critical issue in photopolymerization is nonuniformity. A key measure of nonuniformity is the degree to which monomer conversion varies with depth in the layer.

Figures 1−3 show that for $\beta \leq 1$ significant monomer remains unconverted at each depth, even when the photoinitiator has been completely consumed everywhere. When monomer conversion is incomplete, the final distribution $S_M(z,\infty)$ always has its maximum at $z = 0$ and decays monotonically toward the rear of the layer. The difference $\Delta_M = S_M(0,\infty) - S_M(1,\infty)$ represents

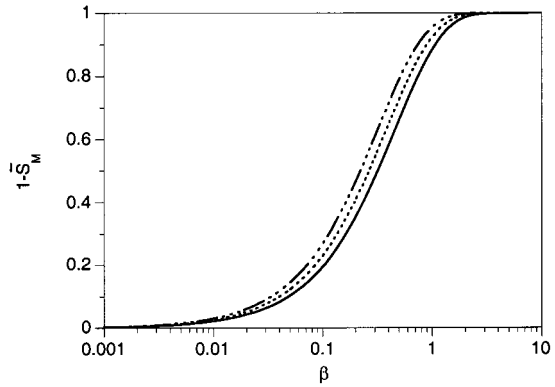

Figure 6. Dependence of the final overall dimensionless monomer conversion $1 - \bar{S}_M(\infty)$ on β: (—) $\gamma = 1$; (· · ·) $\gamma = 5$; (—· · ·—) $\gamma = 100$.

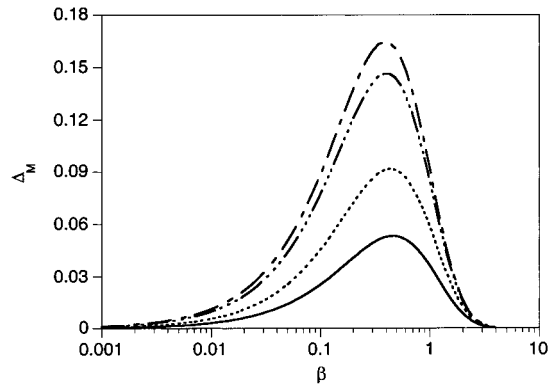

Figure 7. Dependence on β of the spatial nonuniformity in final overall dimensionless monomer conversion on β for $\Delta_M(\beta,\gamma) = S_M(0,\infty) - S_M(1,\infty)$ on β: (—) $\gamma = 1$; (· · ·) $\gamma = 2$; (—· · ·—) $\gamma = 5$; (— - —) $\gamma = 100$.

the degree of nonuniformity across the layer, which we compute from

$$\Delta_M(\beta,\gamma) = S_M(0,\infty) - S_M(1,\infty) = e^{-2\beta} - \exp\left\{-\frac{2\beta \arctan[(e^{\gamma}-1)^{1/2}]}{(1-e^{-\gamma})^{1/2}}\right\} \quad (21)$$

Equation 21 shows that Δ_M vanishes as $\beta \to 0$, in which limit termination is so much faster than propagation that essentially no monomer conversion occurs, and as $\beta \to \infty$, in which case propagation is so fast that all monomer at each depth is converted. For each initial absorbance γ, Δ_M must therefore attain its maximum at some intermediate β, as seen in Figure 7, which shows how Δ_M depends on β for several values of γ. For each β, the degree of nonuniformity increases monotonically with γ, as indicated in the discussion of monomer conversion profiles above.

Differentiation of (21) with respect to β shows that for any γ, the maximum Δ_M occurs for

$$\beta_{max} = \frac{1}{2}\left\{\frac{\arctan[(e^{\gamma}-1)^{1/2}]}{(1-e^{-\gamma})^{1/2}} - 1\right\}^{-1} \ln\left\{\frac{\arctan[(e^{\gamma}-1)^{1/2}]}{(1-e^{-\gamma})^{1/2}}\right\} \quad (22)$$

It is easily shown that β_{max} ranges from $\ln(\pi/2)/(\pi - 2) = 0.3956...$ as $\gamma \to \infty$, to $^1/_2$ as $\gamma \to 0$, with the maximum value of Δ_M at each γ being given by $\Delta_{M,max}(\gamma) = (1 - 1/\sigma)\sigma^{1/(1-\sigma)}$, where $\sigma = (1 - e^{-\gamma})^{1/2} \arctan[(e^{\gamma} - 1)^{1/2}]$. A simple limiting process applied to (21) shows that $\Delta_{M,max}(\gamma) \to (\pi/2 - 1)(2/\pi)^{\pi/(\pi-2)} = 0.1647...$ as $\gamma \to \infty$.

From these results, it follows that the spatial variation of $S_M(z,\infty)$ does not exceed 0.1647 regardless of β and γ and that, for $\beta < 0.02$ and $\beta > 2$, Δ_M will not exceed 0.02, regardless of γ.

Temporal Variation of Layer-Averaged Monomer Conversion. The results presented so far show the spatiotemporal variation of monomer concentration as a function of fractional consumption of photoinitiator or fractional conversion of monomer and the final conversion of monomer as a function of β and γ. As such, they provide no direct information about the rate of monomer conversion. Here, we show how the fractional conversion of monomer, $1 - \bar{S}_M(\tau)$, depends on dimensionless time for a range of β and γ.

For $\beta = 10^{-3}$, 0.1, 1, 10, and 100, Figure 8a–e shows the dependence of $1 - \bar{S}_M$ on τ for $\gamma = 1$, 10, 50, and 100. For $\beta = 10^{-3}$, at which the final fractional conversion barely exceeds 0.3% at the highest initial absorbance, the dimensionless time $\tau = \phi I_0 \alpha_A t$ required to achieve essentially final conversion at each γ increases with γ and is nearly equal to γ for $\gamma \geq 10$. If one thinks of the initial absorbance as being proportional to the layer thickness L, a quantity which does not enter into the definitions of β and τ, then it is perfectly natural for conversion time to depend approximately linearly on γ. We also note that, especially at higher γ, overall progress of the reaction is essentially linear in time until conversion of monomer has nearly reached its final value.

As β increases, so does the final degree of conversion, as noted above. For $\beta = 0.1$, Figure 8b shows that $1 - \bar{S}_M(\infty)$ ranges from slightly less than 0.2 at $\gamma = 1$ to slightly more than 0.25 at $\gamma = 100$ and that again the time for completion is approximately equal to γ for $\gamma \geq 10$. The generally weak dependence of conversion time on β, particularly at high initial absorbances, is associated with the fact that, at high values of γ, the rate-limiting step is penetration of light into the layer rather than the kinetics of the termination and propagation reactions.

By $\beta = 1$, final conversions are on the order of 90% and nearly independent of γ for $\gamma \geq 1$. Figure 8c–e shows that, beginning with this value of β, initial curvature is apparent in conversion vs time histories for higher values of γ and becomes more pronounced as β increases. For $\beta = 10$ and 100, the $\gamma = 50$ and 100 curves are essentially tangent to the vertical axis at $\tau = 0$, before assuming the slopes they had at $\beta = 0.1$. This curvature is due to the fact that initial absorption of photons, near $z = 0$, leads to photoinitiation at a higher monomer concentration than remains at downbeam locations through which the front later passes. This initial photoinitiation gives rise to high primary radical concentrations, and greater initial monomer conversion rates as β increases, due to a higher ratio of the propagation to termination rate constants. As the photoinitiation front moves deeper into the layer, a steady traveling-wave state is reached, with some monomer having been converted downbeam of the front (due to photopolymerization initiated by slow absorption and initiation downbeam of the front), where the primary radical concentration is low and termination is therefore rare.

Figure 9a–e show how $-d\bar{S}_M/d\tau$ varies with fractional photoinitiator consumption. The latter is a useful

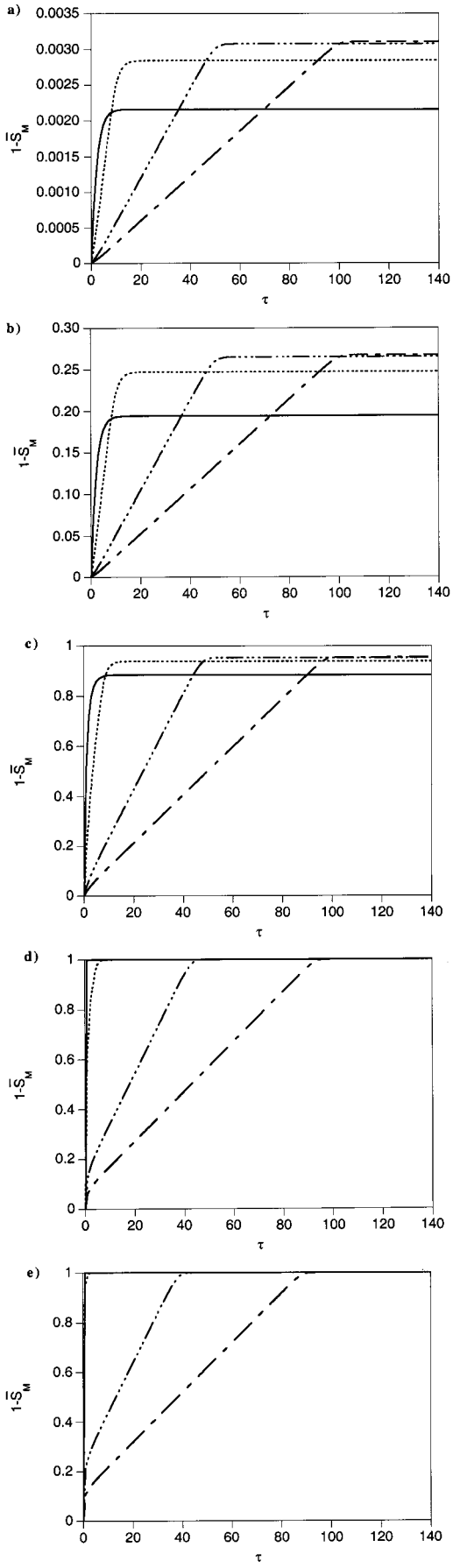

Figure 8. Temporal variation of the dimensionless monomer conversion $1 - \bar{S}_M$: (—) $\gamma = 1$; (· · ·) $\gamma = 10$; (—· · ·—) $\gamma = 50$; (— - —) $\gamma = 100$. (a) $\beta = 10^{-3}$; (b) $\beta = 0.1$; (c) $\beta = 1$; (d) $\beta = 10$; (e) $\beta = 100$.

independent variable for two reasons. First, since characteristic monomer conversion times depend strongly on γ (see Figure 8a−e), this choice allows for comparison of photopolymerizations with different time scales. Second, $1 - \bar{S}_A$ increases monotonically with τ, and for large γ increases nearly linearly with τ until photoinitiator is nearly completely consumed. For $\beta = 10^{-3}$, Figure 9a shows that for small γ, $-d\bar{S}_M/d\tau$ decreases monotonically as initiator is consumed (i.e., monotonically in time). By $\gamma = 10$, however, the rate passes through a maximum near 50% photoinitiator consumption, before ultimately decreasing to zero as all photoinitiator is consumed. At large γ (50 and 100), $-d\bar{S}_M/d\tau$ is almost constant over the entire course of the reaction, corresponding to nearly steady propagation of the traveling-wave solution through the layer. The initial increase in monomer conversion rate is a consequence of the initially high radical chain concentration near $z = 0$, as discussed above in connection with spatiotemporal variation of the monomer concentration, shown in Figures 2 and 3. For $\gamma = 10$ and 100, parts c and d of Figure 3, respectively, show that the extent of monomer conversion near the wall, which occurs during the initial transient, is lower than under downbeam conditions of lower radical chain concentration. For all β and γ, the decrease in rate as $\bar{S}_A \rightarrow 0$ is associated with the fact that our model predicts that monomer conversion ceases when all photoinitiator has been consumed.

Comparison of parts a (for $\beta = 10^{-3}$) and b ($\beta = 0.1$) of Figure 9 shows that if the rates are divided by β, the variation with $1 - \bar{S}_A$ is nearly identical at each γ. This follows from the fact that, for these small values of β, so little monomer is converted (see Figure 6) that the departure of the dimensionless monomer concentration from unity on the right-hand side of (15) is sufficiently small that the right-hand side is closely approximated by the product of its first two factors.

Figure 9c shows that for $\beta = 1$, initial increases in $-d\bar{S}_M/d\tau$ for $\gamma \geq 10$ have been replaced by initial decreases, the magnitudes of which increase with increasing γ. These decreases, which become more pronounced as β increases, are associated with "beyond-the-front" photoinitiation, which at large β and γ gives rise to very low radical chain concentrations and low rates of the termination reaction (6) downbeam of the photoinitiation front. Thus, at $\tau = 0$ ($1 - \bar{S}_A = 0$), the photoinitiation rate decays exponentially away from $z = 0$, with the few primary radicals created far downbeam finding the full monomer concentration available for the creation of radical chains via (4), and the termination reaction (6) having a low overall rate. For large β, the propagation reaction (5) proceeds rapidly, converting significant amounts of monomer at downbeam locations where no significant photoinitiator consumption has yet occurred. This effect is observed, on a spatiotemporal basis, in Figure 10, described below. We also note that for $\gamma = 1$ and 10 the monomer conversion rate decreases significantly as photoinitiator is consumed, whereas for $\gamma = 50$ and 100, there are still wide ranges of $1 - \bar{S}_A$ for which the monomer conversion rate is nearly constant. This results from the fact that for large γ, if β is not so large that beyond-the-front monomer conversion is significant, then the traveling-wave behavior of the photoinitiator consumption[2] will be reflected in traveling-wave conversion of monomer (Figures 1d, 2d, 3d, 4d, and 5d), whereas for smaller γ, photoinitiator consumption and monomer conversion

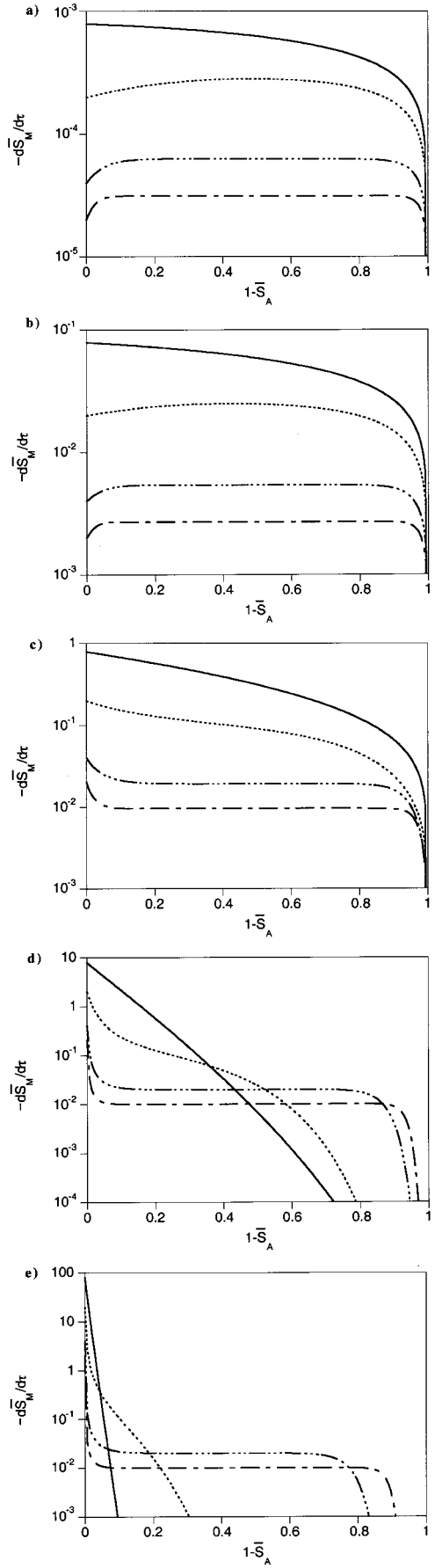

Figure 9. Variation of the dimensionless monomer conversion rate $-d\bar{S}_M/d\tau$ with fractional consumption of initiator $1 - \bar{S}_A$: (—) $\gamma = 1$; (• • •) $\gamma = 10$; (—• • •—) $\gamma = 50$; (— - —) $\gamma = 100$. (a) $\beta = 10^{-3}$; (b) $\beta = 0.1$; (c) $\beta = 1$; (d) $\beta = 10$; (e) $\beta = 100$.

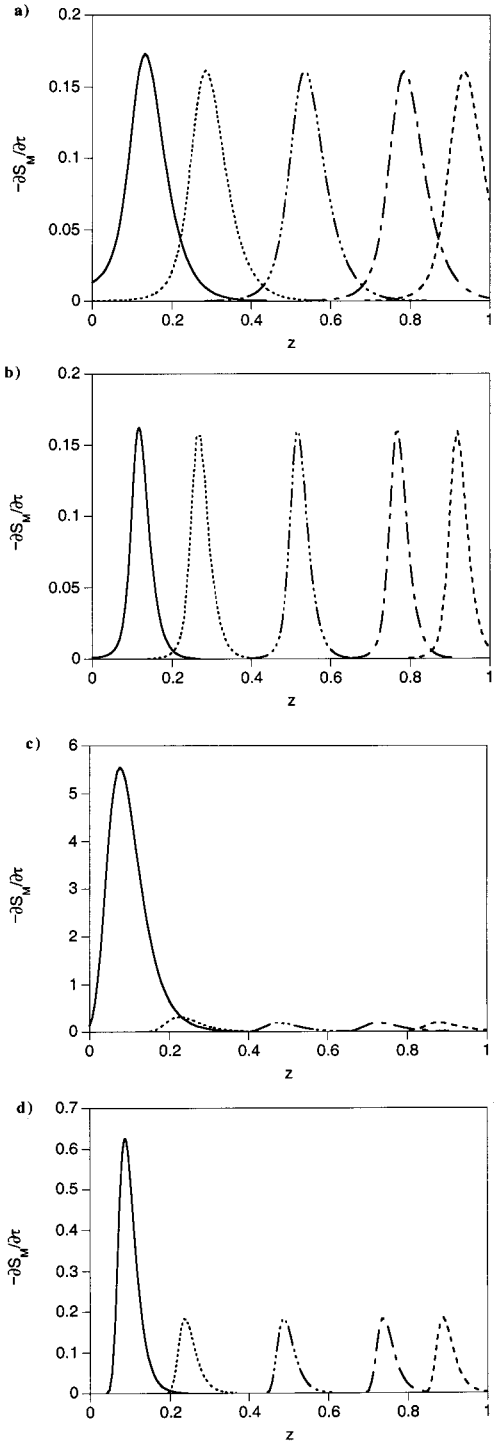

Figure 10. Spatiotemporal variation of the dimensionless monomer conversion rate $-\partial S_M/\partial\tau$ as a function of $z = x/L$ at different degrees of monomer conversion $1 - \bar{S}_M$: (—) $\bar{S}_M = 0.9$; (• • •) $\bar{S}_M = 0.75$; (—• • •—) $\bar{S}_M = 0.5$; (— • —) $\bar{S}_M = 0.25$; (— — —) $\bar{S}_M = 0.1$. (a) $\beta = 1$, $\gamma = 50$; (b) $\beta = 1$, $\gamma = 100$; (c) $\beta = 100$, $\gamma = 50$; (d) $\beta = 100$, $\gamma = 100$.

occur more homogeneously and are less linear in time. Once the steady traveling-wave situation is reached, beyond-the-front monomer conversion leads to much of the photoinitiator absorption and primary radical formation occurring at depths where monomer conversion is already essentially complete. Thus, compared to the situation at $\tau = 0$, where every newly created primary radical encounters the full monomer concentration, the local monomer conversion rate will be much lower.

For large β, Figure 9d,e shows that at large γ the initially high monomer conversion rates decrease very rapidly with increasing photoinitiator consumption, reflecting the transition from the initial situation, in which unconverted monomer exists at its full concentration everywhere that photoinitiator absorbs, to the steady traveling wave, in which much of the absorption by photoinitiator occurs at depths where monomer conversion is nearly complete.

Spatiotemporal Variation of Monomer Conversion Rate. The increasing difference, as β increases, between the initial slope of $1 - \bar{S}_M$ vs τ, compared to the steady traveling-wave value, shown in Figure 8a−e, suggests that photoinitiation in virgin monomer at $\tau = 0$ near $z = 0$ converts monomer much faster than at later times and much faster as β increases at fixed τ.

To examine this more closely, we consider spatiotemporal variation of the monomer conversion rate, $-\partial S_M/\partial\tau$, given by the right-hand side of (15). Figure 10a−d shows that for $\beta = 1$ and 100, and for $\gamma = 50$ and 100, monomer conversion is highly localized at each fractional conversion, with the degree of localization being greater for $\gamma = 100$. For $\beta = 1$ and both values of γ, Figure 10a,b shows that the monomer conversion rate at each fractional conversion is nearly symmetric about its peak, and there is essentially no variation in the layer-integrated rate as the front moves through the layer. For $\beta = 100$, Figure 10c,d shows that the profiles are noticeably asymmetric about their maxima, with the downbeam variation being more gradual. The asymmetry about the maxima at higher β is a result of two factors. First, at higher β, increased monomer conversion occurs downbeam of the propagating front, where photoinitiation rates (and hence radical chain concentrations) are low, but monomer conversion rates are significant due to chain propagation being much faster than termination. This gives rise to the relatively long "tail" in $-\partial S_M/\partial\tau$, most evident in Figure 10d. Second, as β increases, an increasing fraction of the absorption by photoinitiator occurs at depths at which this beyond-the-front polymerization has already converted essentially all of the monomer. Both effects become more important at higher values of β, contributing to increased asymmetry.

Discussion

Mechanistic Sources of Nonuniformity. The above results clearly demonstrate that nonuniform photoinitiation can give rise to monomer conversion profiles with varying degrees of nonuniformity. The instantaneous degree of nonuniformity depends on two dimensionless parameters, β and γ, as well as the extent of monomer conversion. The final degree of nonuniformity depends only on β and γ.

Two related factors contribute to nonuniform monomer conversion. First, attenuation has the effect of spatially localizing photoinitiation, to a degree that increases rapidly with increasing γ.[2] Specifically, photoinitiator consumption is initially more rapid near the optical entrance ($z = 0$) than downbeam, due to attenuation. In fact, the rate of photoinitiator consumption at $z = 0$ and $\tau = 0$ is higher than at any other point at any other time. Second, as a consequence, photoinitiator consumption near the optical entrance initially occurs under conditions of high primary radical and radical chain concentration, resulting in relatively higher rates of the termination reactions (6) than at any point downbeam or at any later time. The result of the higher termination rate is that the number of monomer molecules converted per photon absorbed will be lower in the front of the layer than in the back. This reduces the final conversion of monomer near the front of the layer.

Relationship to Applications. Reference to Figure 6 shows that the final conversion of monomer depends strongly on β, and that to achieve nearly complete conversion, β must exceed unity, to an extent that decreases with increasing initial absorbance γ. For β in excess of about 2, conversion will be nearly complete regardless of the initial absorbance. From (17), we see that, for fixed values of the rate constants k_p and k_t and photophysical parameters α_A and ϕ, the parameter β is proportional to the square root of the ratio of initial photoinitiator concentration $C_{A,0}$ to the incident light intensity I_0. Increasing this ratio can be accomplished by increasing $C_{A,0}$, with the added benefit that the resulting increase in γ also increases conversion (Figure 6). The penalty is increased use of photoinitiator. On the other hand, decreasing I_0 will have the generally desirable result of reducing the degree of thermal nonuniformity across the layer, with the penalty of increased processing time. The choice will necessarily depend on the application.

We also note that if the absorption coefficient and initial concentration of the photoinitiator, and the quantum yield of photoinitiator consumption are known, then β can be determined at each light intensity from a measurement of the conversion $1 - \bar{S}_M(\infty)$. If f is also known, then the ratio $k_p/k_t^{1/2}$ can be estimated at each light intensity from the final overall conversion. Comparison of the light intensity dependence of the extracted value of $k_p/k_t^{1/2}$ to the predictions shown in Figure 6 will reveal the extent to which kinetics depart from the assumptions of our model and provide guidance to the development of more sophisticated models accounting for other effects, such as the dependence of kinetic parameters on the chain length distribution and the degree of monomer conversion. Figure 6 shows that the extraction of β from the final overall conversion is best accomplished in the range $0.07 < \beta < 0.7$, for which the sensitivity of conversion to β is greatest.

Figure 6 also shows that a minimum value of β of about 2 is required to ensure nearly complete conversion of monomer, essentially independent of γ. From this and the definition (17), we see that for known values of the rate constants, absorption coefficient, quantum yield, and f, complete conversion of monomer will be ensured if the incident light intensity and photoinitiator concentration satisfy the relation

$$\frac{C_{A,0}}{I_0} > \frac{4\phi k_t \alpha_A}{f k_p^2} \tag{23}$$

From the spatiotemporal variation of monomer conversion rates shown in Figure 10a−d, we can infer that the distribution of molecular weights in the photopolymerized material will vary significantly within the layer. In the front of the layer, where monomer is converted at higher radical concentrations than elsewhere, we expect shorter chains, and smaller fractions of the monomer to be incorporated into high molecular weight chains, with the magnitude of the effect increasing with both β and γ. As a consequence, polymer properties depending on the molecular weight distribution will vary along the propagation direction.

Relationship to Previous Work. A recent computational simulation by Goodner and Bowman[5] considered a one-dimensional unsteady photopolymerization model accounting for attenuation and photoinitiator consumption, and incorporating a kinetic scheme allowing for diffusion-limited propagation and termination at high degrees of monomer conversion. They analyzed polymerization of 3 mm layers of 2-hydroxyethyl methacrylate at two concentrations of an initiator (2,2-dimethoxy-2-phenylacetophenone; DMPA) for which the absorbance of the layer is unchanged during the course of the reaction, and at one concentration of a fictitious initiator with the same absorption coefficient as DMPA, but which undergoes complete photobleaching. Contour plots of photopolymerization rate and one plot of fractional conversion of monomer showed clear evidence of nonuniformity at high initiator rates. None of these results showed evidence of a traveling-wave solution with an asymptotically constant wave speed. While the cause of this is clear for nonbleaching DMPA, the cause is less clear for the fictitious photobleached initiator case, with initial absorbance $\gamma = 22.5$.

Mateo et al.[18] demonstrated that the initial rate of photopolymerization of methyl acrylate initiated by 4-(dimethylamino)-4′-isopropylbenzophenone was proportional to the square root of the incident light intensity. For "unstirred" cases (i.e., with no mass transfer), they also showed that as the photoinitiator concentration increased, the initial rate increased, passed through a maximum near $C_{A,0} = 6.1 \times 10^{-5}$ M, and then decreased. From (12) and (14), we see that the monomer conversion rate averaged over the layer thickness, $\bar{R}_p(t)$, is given at the initial time by

$$\bar{R}_p(0) = k_p\sqrt{f\phi C_{A,0}\alpha_A I_0/k_t}\,\frac{C_{M,0}}{L}\int_0^L e^{-\alpha_A C_{A,0}x/2}\,dx \qquad (24)$$

which is equivalent to (1) for $f = 2$. From this, it follows that the maximum of $\bar{R}_p(0)$ occurs when

$$\alpha_A C_{A,0} L - e^{\alpha_A C_{A,0} L/2} + 1 = 0 \qquad (25)$$

From this, it is easily shown that the maximum initial rate occurs when $\gamma = 2.5128...$, a result obtained by Lissi and Zanocco,[33] who, however, did not note the restriction to initial rates. If we use the molar absorption coefficient ($\epsilon_A = 3800$ M^{-1} cm^{-1}) given by Mateo et al.[18] for the photoinitiator, the path length $L = 4.138$ cm (corresponding to the length of the cylindrical reactor), and $C_{A,0} = 6.1 \times 10^{-5}$ M, we get the slightly lower value of $\gamma = 2.21$.

Several factors might contribute to this 12% discrepancy. First, for the "unstirred" experiments, two numerical values of the "incident light intensity" were reported (with the units of a volumetric photon absorption rate) in the caption of Table 3 of ref 18, so that it is impossible to unambiguously determine the light intensity in any single experiment. Second, we took the photoinitiator concentration giving the maximum integrated initial rate to be 6.1×10^{-5} M, the value at which the largest initial rate was reported. The gaps between that value and the next-closest photoinitiator concentrations (1.1×10^{-4} and $\sim 1 \times 10^{-5}$ M) are quite large, allowing for considerable uncertainty in the value of $C_{A,0}$ at which $\bar{R}_p$ attains its maximum value. Third, it is unclear whether the beam propagates along the cylinder axis (as assumed here) or in another direction, calling the value of L into some doubt. Finally, the "initial rates" reported by Mateo et al. correspond to integrated rates over the first 2−4% of conversion (with the conversion in each experiment unreported) rather than to true differential rates at $t = 0$. The decrease of $\bar{R}_p$ with time (see Figure 9), although smaller for these small values of β ($\beta \sim 0.1$ in the experiments of Mateo et al.) than at larger β, may still contribute significantly to the 12% discrepancy in the value of γ at which $\bar{R}_p$ is maximized. Given all of these uncertainties, the 12% agreement between the computed and experimental values is quite good.

We note that our model predicts that the final layer-averaged extent of monomer conversion decreases monotonically with increasing light intensity, corresponding to decreasing β. As discussed above, decreasing β leads to a concomitant increase in radical concentrations and hence higher termination rates. In systems where absorption by the photoinitiator or other species leads to significant heating, however, the temperature dependence of the propagation rate constants and diffusion coefficients can lead to increases in the final conversion as I_0 increases.[28]

Dependence on Monomer Concentration. Like previous photopolymerization models, ours predicts that fractional conversion of monomer is independent of the initial monomer concentration $C_{M,0}$. This result follows directly from the linear differential eq 12 for the monomer concentration or its dimensionless counterpart (15). If the steady-state approximation had not been made, the governing equations would be the nonlinear system (7a−d), in which the rate of change of monomer concentration would be proportional to the product of the monomer concentration and the total radical concentration. Since the rate of change of the latter is independent of the former (see (10)), the monomer conversion rate would still depend linearly on monomer concentration, even if the steady-state approximation was not made. Hence, the lack of dependence of the fractional conversion of monomer on $C_{M,0}$ is a property of the full set of governing equations (7a−d) and is not an artifact of the steady-state approximation.

On the other hand, we expect that in real free-radical polymerizations a number of properties will depend on the initial monomer concentration. One such property is the molecular weight distribution, which in our model is determined by the rates of the termination reactions (6). Since the concentrations of the individual radical species depend on C_M (through (7b) and (7c)), so too will the rates of the constituent reactions of (6). Thus, since the rates of the termination reactions are proportional to the products of pairs of radical concentrations, it is clear that the molecular weight distribution will shift to higher molecular weights as the initial monomer concentration increases with all other parameters (including initial photoinitiator concentration) held constant. In systems where attenuation is important, we also expect that the molecular weight distribution will vary from point to point. At large values of β, the final molecular weight distributions will be shifted downward near $z = 0$ compared to farther downbeam, due to significant "beyond-the front" polymerization at low radical concentrations.

Incorporation of More Complex Kinetic Behavior. The assumption that the propagation and termination rate constants are independent of conversion and chain length is a reasonable one in liquid solution, with

the variation of k_p and k_t being fairly modest. In such systems, the predictions of the present analysis can be expected to be reasonably accurate over a wide range of conversion. However, in bulk photopolymerizations, it is well-known that k_p and k_t can decrease significantly during the course of reaction. Typically, the ratio $k_p/k_t^{1/2}$ increases with conversion due to the "gel effect" and then decreases with increasing conversion. In such systems, the results of the present analysis are likely to be qualitatively correct for small conversions and to become increasingly inaccurate as the degree of conversion increases. Quantitative prediction of high-conversion behavior in bulk photopolymerizations will thus require use of conversion-dependent rate constants in the kinetic model (7a−e). To the extent that k_p and k_t depend on the local molecular weight distribution (rather than simply on the local degree of monomer conversion), this (or any other) model will require considerably more kinetic data than is available for most systems.

Finally, we note that at sufficiently high incident light intensities, the induction period required for the total radical concentration (governed by eq 10) to achieve the steady-state balance (11) between the rate of creation of primary radicals and the bimolecular termination rate of all radicals may be so long[34] that it is comparable to or exceeds the time necessary to completely convert the monomer. In that event, the steady-state approximation (11) will break down, and we will have to solve (7d) and (10) rather than simply (12). This will lead to introduction of two additional dimensionless parameters (say, $C_{A,0}/C_{M,0}$ and $k_tC_{M,0}/(\phi I_0\alpha_A)$ beyond β and γ, since in this case k_p and k_t no longer appear simply as the ratio $k_p/k_t^{1/2}$, and the monomer concentration no longer "cancels out". According to (10), the total radical concentration will initially grow at a rate proportional to I_0, so that if the induction period is not short compared to the conversion time, the average monomer conversion rate will depend more strongly on I_0 than the square-root dependence predicted by (12). This breakdown of the steady-state assumption (and the resulting dependence of the monomer conversion rate on the square root of the incident light intensity specified by eq 12) is a means by which monomer conversions higher than those shown in Figure 6 can be achieved at small β.

Conclusions

For free-radical photopolymerization, we have shown how the local monomer conversion rate depends on position and time over the entire range of initial absorbance, $\gamma = \alpha_A C_{A,0} L$, and over a wide range of a second dimensionless parameter, $\beta = k_p[fC_{A,0}/(\phi\alpha_A I_0 k_t)]^{1/2}$. For β lying below ≈2, monomer conversion will be measurably incomplete, to a degree that decreases with increasing β and γ. For larger β, nearly complete conversion of monomer occurs at every value of γ. The extent of nonuniformity in the final monomer conversion approaches zero for small and large β, for which essentially no monomer is converted and essentially all monomer is converted, respectively. A maximum is achieved at an intermediate β, whose value depends on γ. For large values of the initial absorbance, monomer conversion occurs as a traveling wave propagating with an essentially steady speed after an initial transient. For large values of β and the initial absorbance, the initial monomer conversion rate is much higher than the steady traveling-wave rate.

Acknowledgment. We are grateful to two anonymous reviewers for comments that materially improved this paper. Pacific Northwest National Laboratory is operated by Battelle for the U.S. Department of Energy under Contract DE-AC06-76RLO 1830. The authors gratefully acknowledge additional support of this work by NSF Grants MSM-8451157, CTS-9017181, and CTS-9613241.

References and Notes

(1) Flory, P. J. *Principles of Polymer Chemistry*; Cornell University Press: Ithaca, NY, 1953; p 114.
(2) Terrones, G.; Pearlstein, A. J. *Macromolecules* **2001**, *34*, 3195−3204.
(3) Decker, C. *Prog. Polym. Sci.* **1996**, *21*, 593−650.
(4) De Lange, C.; Bausch, J. R.; Davidson, C. L. *J. Oral Rehabil.* **1980**, *7*, 369−377.
(5) Goodner, M. D.; Bowman, C. N. In *Solvent-Free Polymerizations and Processes. Minimization of Conventional Organic Solvents;* ACS Symposium Series 713; Long, T. E., Hunt, M. O., Eds.; American Chemical Society: Washington, DC, 1998; pp 220−231.
(6) Ruyter, I. E. *Acta Odontol. Scand.* **1981**, *39*, 27−32.
(7) Cook, W. D. *J. Macromol. Sci., Chem.* **1982**, *A17*, 99−111.
(8) Cook, W. D. *J. Dent. Res.* **1980**, *59*, 800−808.
(9) Cook, W. D.; Standish, P. M. *Austral. Dent. J.* **1983**, *28*, 307−311.
(10) Cook, W. D. *J. Appl. Polym. Sci.* **1991**, *42*, 2209−2222.
(11) Hirose, T.; Wakasa, K.; Yamaki, M. *J. Mater. Sci.* **1990**, *25*, 1209−1213.
(12) Odian, G. *Principles of Polymerization*, 3rd ed.; Wiley: New York, 1991.
(13) We have modified eq 3-65 of ref 12 to match parentheses. That eq 3-65 of ref 12 must be the layer integrated average rate, rather than the layer integrated overall rate, is inferred from the fact that the symbol, R_p, on the left-hand side, is identical to that used for the local rate in eq 3-59.
(14) Joshi, M. *J. Appl. Polym. Sci.* **1981**, *26*, 3945−3946.
(15) Anseth, K. S.; Newman, S. M.; Bowman, C. N. In *Biopolymers II*; Advances in Polymer Science; Peppas, N. A., Langer, R. S., Eds.; Springer: New York, 1995; Vol. 122, pp 177−217.
(16) Lindén, L.-Å. In *Radiation Curing in Polymer Science and Technology*; Fouassier, J. P., Rabek, J. F., Eds.; Elsevier Applied Science: London, 1993; Vol. 4, pp 387−466.
(17) Bland, M. H.; Peppas, N. A. *Biomaterials* **1996**, *17*, 1109−1114.
(18) Mateo, J. L.; Bosch, P.; Vázquez, E.; Sastre, R. *Makromol. Chem.* **1988**, *189*, 1219−1227.
(19) Shultz, A. R.; Joshi, M. G. *J. Polym. Sci., Polym. Phys. Ed.* **1984**, *22*, 1753−1771.
(20) Ivanov, V. V.; Decker, C. *Polym. Int.* **2001**, *50*, 113−118.
(21) Allcock, H. R.; Lampe, F. W. *Contemporary Polymer Chemistry*, 2nd ed.; Prentice Hall: Englewood Cliffs, NJ, 1990.
(22) North, A. M. *The Kinetics of Free Radical Polymerization*; Pergamon: Oxford, 1966.
(23) Krongauz, V. V. In *Processes in Photoreactive Polymers*; Krongauz, V. V., Trifunac, A. D., Eds.; Chapman and Hall: New York, 1994; pp 185−259.
(24) Brulle, Y.; Bouchy, A.; Valance, B.; André, J. C. *J. Photochem. Photobiol. A: Chem.* **1994**, *83*, 29−37.
(25) Frazier, D. O.; Hung, R. J.; Paley, M. S.; Long, Y. T. *J. Cryst. Growth* **1997**, *173*, 172−181.
(26) We use the absorption coefficient (ref 27, p 21) for simplicity; it is related to the (decadic) molar absorptivity or extinction coefficient ϵ_A by $\alpha_A = \epsilon_A \ln 10$.
(27) Calvert, J. G.; Pitts, J. N. *Photochemistry*; Wiley: New York, 1966; pp 640−641.
(28) Decker, C.; Bendaikha, T.; Decker, D.; Zahouily, K. *Polym. Prepr.* **1997**, *38*, 487−488.
(29) Wegscheider, R. *Z. Phys. Chem.* **1923**, *103*, 273−306.
(30) Bowman, C. R.; Peppas, N. A. *Macromolecules* **1991**, *24*, 1914−1918.
(31) Hutchinson, R. A.; Beuermann, S.; Paquet, D. A.; McMinn, J. H. *Macromolecules* **1997**, *30*, 3490−3493.
(32) Terrones, G.; Pearlstein, A. J. *J. Am. Chem. Soc.* **1991**, *113*, 2132−2140.
(33) Lissi, E. A.; Zanocco, A. *J. Polym. Sci., Polym. Chem. Ed.* **1983**, *21*, 2197−2202.
(34) Benson, S. W. *J. Chem. Phys.* **1952**, *20*, 1605−1612.

MA010678E